ISRAEL JOURNAL OF
CHEMISTRY
Vol. 32, No. 4, 1992

PRIMARY EVENTS IN PHOTOSYNTHESIS: PROBLEMS, SPECULATIONS, CONTROVERSIES, AND FUTURE TRENDS

M. Bixon,[a] J. Fajer,[b] G. Feher,[c] J.H. Freed,[d] D. Gamliel,[e] A.J. Hoff,[f] H. Levanon,[e] K. Möbius,[g] R. Nechushtai,[h] J.R. Norris,[i] A. Scherz,[j] J.L. Sessler,[k] and D. Stehlik[g]

Institute for Advanced Studies, The Hebrew University of Jerusalem, Jerusalem 91904, Israel

[a]School of Chemistry, Tel Aviv University, Ramat Aviv, Tel Aviv 69978, Israel.
[b]Department of Applied Science, Brookhaven National Laboratory, Upton, NY 11973, USA.
[c]Department of Physics, University of California, La Jolla, CA 92093, USA.
[d]Department of Chemistry, Cornell University, Ithaca, NY 14853, USA.
[e]The Farkas Center for Light-Induced Processes, The Hebrew University, Jerusalem 91904, Israel.
[f]Huygens Labratory, State University of Leiden, 2300 RA Leiden, The Netherlands.
[g]Institute of Experimental Physics, Free University Berlin, D-1000 Berlin 33, Germany.
[h]Department of Botany, The Hebrew University, Jerusalem 91904, Israel.
[i]Chemistry Division, Argonne National Labratory, Argonne, IL 60439, USA.
[j]Department of Biochemistry, The Weizmann Institute of Science, Rehovot 76100, Israel.
[k]Department of Chemistry and Biochemistry, University of Texas at Austin, Austin, TX 78712, USA.

ISRAEL JOURNAL OF
CHEMISTRY
Vol. 32, No. 4, 1992

PRIMARY EVENTS IN PHOTOSYNTHESIS: PROBLEMS, SPECULATIONS, CONTROVERSIES, AND FUTURE TRENDS

Institute for Advanced Studies, The Hebrew University of Jerusalem, Jerusalem 91904, Israel

tainly, a key ingredient missing in the quest to understand the excited state is this lack of direct structural information. Thus an important new area of experimental and theoretical chemistry would be the ability to probe the structure and quantum theory of excited states and reactive chemical intermediates.

In summary, of the many problems that will occur, especially in diffraction studies of single crystals, the following four seem the most severe: (1) the ideal X-ray shutter for providing X-ray pulses is not yet available; (2) complete and/or uniform excitation of the sample is difficult; (3) selection of proper samples for studying dynamic structural changes is not easy, especially when using single crystals; and (4) optical (i.e., visible radiation) excitation of the sample generates heat and shockwaves. Of the four problems perhaps (4) is the most severe barrier to overcome. Hopefully, all these problems have solutions. Regardless, it seems clear that time-dependent X-rays will become a structural probe of increasing utility and value.

7.2 NEUTRON DIFFRACTION, AN ASSESSMENT (A.J.H)

X-ray diffraction yields the positions of skeleton atoms of organic (macro) molecules, but not of the hydrogens attached to the skeleton. Yet, the hydrogens are most probably of prime importance for the details of electron transport, and it is desirable to know their positions accurately. Neutron diffraction, which has a high scattering cross-section precisely for hydrogens, would potentially solve this problem. Pilot experiments have recently been performed on large crystals of lysozyme and hemoglobin.[2a-2c] The results prove that neutron diffraction on large biological molecules is possible to a resolution of 2.0 Å (lysozyme) and 3.0 Å (hemoglobin). On the other hand, these experiments have demonstrated that such resolution is only achieved for large crystals (volumes were 10 and 40 mm^3 for lysozyme and hemoglobin, respectively) with a reasonably small unit cell (lysozyme 270 nm^3, hemoglobin 620 nm^3), while data collection with a strong neutron source took as long as two months for hemoglobin. Some improvement can be achieved by cooling the crystal to cryogenic temperatures, by deuterium exchange, and by enlarging the detector area (about 20-fold improvement is foreseen).

Taking into account the small dimensions and large unit cells of crystals of reaction centers, it is estimated that for usable neutron diffraction data one needs improvement by a factor of more than 6000. Thus, it is unlikely that in the foreseeable future neutron diffraction will be a viable technique for obtaining structural data on photosynthetic reaction centers.

7.3 MAGNETIC RESONANCE

7.3.1 HIGH-FIELD EPR/ENDOR (J.H.F. AND K.M.)

(a) Introduction

As was pointed out in Section 3.2.1, small g-factor differences for different magnetic "sites" or small g-factor anisotropies of the pigment radicals lead to strongly overlapping EPR lines at conventional X-band spectroscopy (9.5 GHz) for which even ENDOR/TRIPLE does not result in well-resolved spectra. This is a common situation for photosynthetic preparations, in particular for the primary donor cation radical in RCs. In analogy to modern NMR spectroscopy, this problem can, in principle, be overcome by applying higher and higher magnetic fields. The increased Zeeman interaction ultimately leads, even for powder-type samples, to a complete separation of spectral features belonging to different principal values of the g-tensor. In addition to the improved Zeeman magnetoselection, high-field EPR is distinguished by its high detection sensitivity for small single crystals (high filling factor, see below). Another advantage of high-field EPR is the transformation of motionally narrowed spectra ($\omega_e \tau_R << 1$) into the slow-motion regime ($\omega_e \tau_R \geq 1$) with increased spectral sensitivity to motional dynamics (ω_e is the Zeeman angular frequency and τ_R is the correlation time of the motion). High-field ENDOR has the additional advantage of allowing single-crystal-like spectra to be taken even from disordered solid state samples with small g-factor anisotropy, and of separating those ENDOR spectra from nuclei with different magnetic moments which overlap at X-band frequency.

Thanks to modern developments in ultra-high-frequency microwave technology, high-frequency/high-field EPR spectrometers were built in various laboratories working, for instance, at 250 GHz ($\lambda \approx 1$ mm, $B_o \approx 9$ T for $g = 2$),[3] at about 150 GHz ($\lambda \approx 2$ mm),[4a,5a] at 95 GHz ($\lambda \approx 3$ mm),[6-8] or at 70 GHz ($\lambda \approx 4$ mm).[9] So far the extension to ENDOR has been established up to the 3-mm band,[6] but an ENDOR setup appears feasible also in the 1-mm band.

(b) Experimental Realizations and First Applications

The high frequencies involved in the mm-wave EPR spectrometers have approached the upper limit of standard technology for microwave components such as detectors, circulators, etc., and are even going beyond it. As examples of recent mm-EPR constructions, the main features of the 1-mm EPR spectrometer at Cornell[3] and the 3-mm EPR/ENDOR spectrometer at Berlin[6] will be briefly described:

In the Cornell EPR spectrometer, the microwave source is a phase-locked Gunn diode that is frequency tripled to 250 GHz with 3 mW output power. The main superconducting magnet coil has a maximum field of 9.2 T, and an

auxiliary superconducting field-sweep coil can be swept ±54 mT while the main coil is persistent. In this way, the spectrometer is similar in the operation of the magnet to a conventional EPR spectrometer. The maximum sweep rate is 3.5 mT/sec in either direction. The field homogeneity is better than 3 ppm in a 1-cm-diameter spherical volume, and the field persistence at 9 T is at least 10^{-7}/h. The maximum field modulation is 5 mT at 80–100 kHz. The room temperature bore diameter is 44 mm. The far infrared (FIR) detector is a GaAs Schottky diode, optimized for use at 250 GHz. It is the noise limiting component. At such high frequencies, waveguide losses preclude propagating the radiation between the source and the detector by waveguide. Instead, quasioptical techniques of the FIR have been employed in the spectrometer with a Fabry–Perot resonator operating in the *transmission* mode. Thus, the 1-mm beam travels from the source through a series of focusing lenses to a Fabry–Perot resonator, and similarly from the resonator to the detector, with only minor losses in signal intensity. The detected EPR signal at the field modulation frequency is then processed as in a standard EPR spectrometer to obtain the first-derivative signal.

The sensitivity of the 1-mm spectrometer is estimated, in terms of minimum number of observable spins, to be 10^{12} spins for an EPR linewidth of 0.1 mT, unsaturated at the available 3 mW of incident microwave power, and 1 s time constant of the lock-in amplifier.[3] The high resolution of the 1-mm EPR spectrometer for nitroxide radical spectra in the rigid-limit has been demonstrated taking PDT as an example[3] (PDT is 2,2',6,6'-tetramethyl-4-piperidine *N*-oxide (perdeuterated)). The *g*-tensor components can be read directly from the spectrum, and the nitrogen hf coupling is also easily obtained (Fig. 7.2).

The importance of 1-mm EPR for studies of rotational motion has also been clearly demonstrated.[10] Fig. 7.3 shows, for the PDT nitroxide spin probe in toluene-d8, the characteristic features of fast- to slow-motional spectra covering the range of motional correlation times τ_R from about 1 to 100 ps. The spectra for fast motions ($\tau_R < 100$ ps) are found to be much more sensitive to the effects of motion than the corresponding 9 GHz spectra, whereas for $\tau_R \geq 100$ ps the slow-motional regime sets in, which is an order of magnitude faster in the case of 250 GHz EPR vs. 9 GHz EPR. One is therefore able to combine the advantages of fast- vs. slow-motional spin relaxation in a variety of systems by comparative studies at different frequencies.

In the Berlin EPR/ENDOR spectrometer the microwave source (95 GHz, W-band) is either a low-noise Gunn oscillator (6 mW output power) or a klystron (300 mW). The magnetic field is produced by a cryomagnet with a room temperature bore of 88-mm

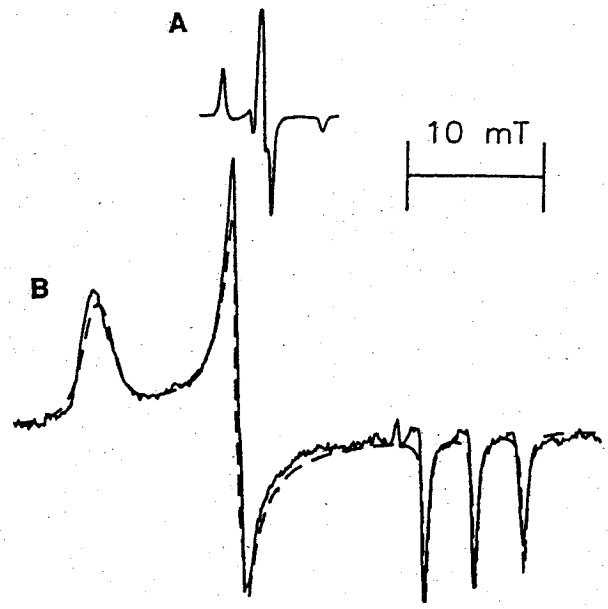

Fig. 7.2. Rigid-limit spectra of 4×10^{-4} M PDT in 25%/75% glycerol-d3/D2O (–100° C) taken at (A) 9.5 GHz and (B) 250 GHz.[3] [PDT is 2,2',6,6'-tetramethyl-4-piperidine *N*-oxide (perdeuterated)] . At 250 GHz, one may simply read off the *g*-values and the nitrogen hf coupling from the rigid-limit spectrum. At X-band, careful simulation would be required to extract the *g*- and *A*-tensors in favorable cases.

diameter and maximum field of 6 T. This bore is large enough to accomodate, besides the EPR probehead, additional components such as ENDOR coils, light-pipe, goniometer etc. The field homogeneity over a sample capillary of 1-mm diameter and 10-mm length is better than 0.01 mT, the long-term field stability is better than 0.001 mT/min, the short-term stability is 10^{-4} mT at a detection time constant of 1 s. The field can be linearly varied with time at a sweep rate from 0 to 50 mT/min full range. Field modulation up to 4 mT_{pp} at 1 kHz can be applied; for ENDOR, additional frequency modulation (20 kHz) and field-frequency locking are employed. To minimize attenuation losses at the W-band frequencies, oversized waveguides are used between microwave bridge and resonator. The resonator incorporating the sample is either of the Fabry–Perot type, with two concave mirrors in almost confocal separation,[6,11] or a cylindrical TE011 cavity; both resonators operate in the *reflection* mode with variable iris coupling to the waveguide.[12,13] The microwave bridge is completed by a circulator and a detector which is either a Schottky diode or a helium-cooled hot-electron InSb bolometer. Liquid or solid samples are studied in thin-walled quartz capillaries; single crystals can be rotated about three orthogonal axes. The sensitivity of the 3-mm EPR spectrometer with the Schottky diode is estimated to be 10^9 spins for non-lossy

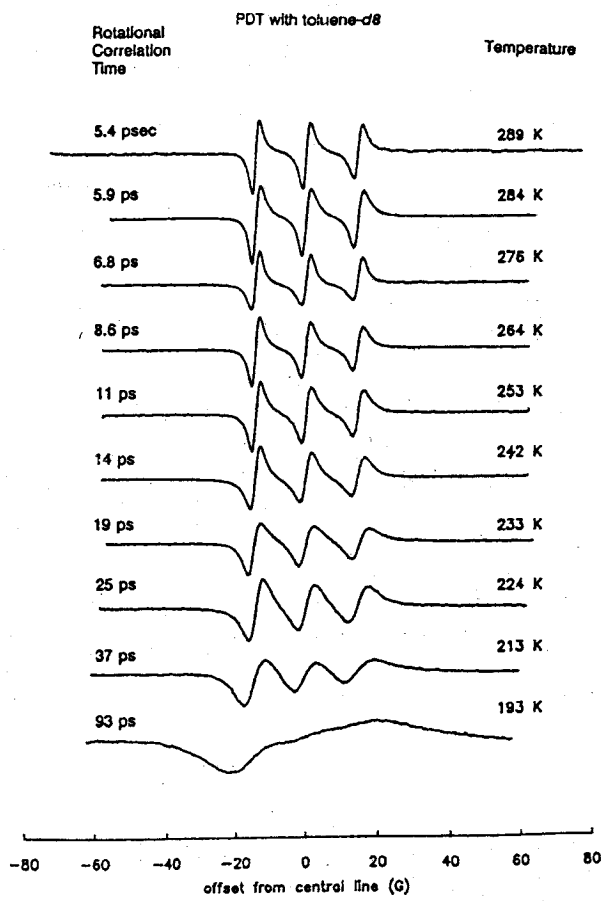

Fig. 7.3. Fast- to slow-motional 250 GHz EPR spectra of PDT spin probe in toluene-d8 in the temperature region 290 K > T > 190 K.[10] These spectra demonstrate the sensitivity of FIR-EPR to molecular reorientations over approximately a decade of rotational correlation times.

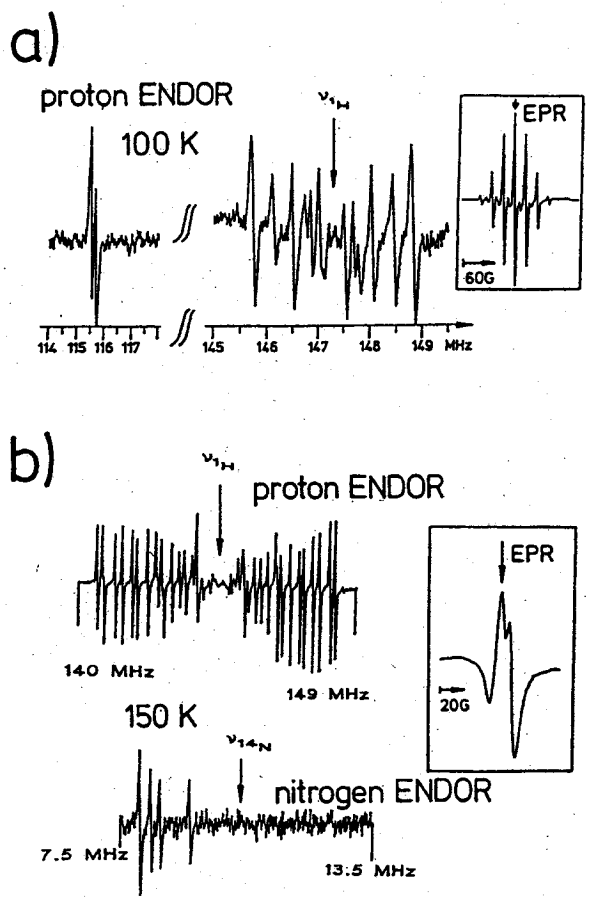

Fig. 7.4. EPR and ENDOR spectra at 3-mm microwave-length (95 GHz, W-band) of single crystals of (a) γ-irradiated α-aminoisobutyric acid with crystal axis $b \parallel B_0$ (ref 6) and (b) of DANO (di-*p*-anisylnitroxide) 1% in 4,4-dimethoxybenzophenone[11] with crystal axis $a \parallel B_0$. The EPR transition on which ENDOR is performed is indicated in the respective EPR spectrum by an arrow. By varying the B_0 field to different parts of the EPR spectrum, selection of different radical sites with different hf interactions can be achieved. From the ENDOR line positions, ν_i^{ENDOR}, the dipolar (A_i) and the quadrupolar (Q_i) hf couplings can be deduced according to $\nu_i^{ENDOR} = |1/2\, A_i \pm \nu_n \pm Q_i|$, where ν_n is the nuclear Zeeman frequency, e.g., ν_{1H} or ν_{14N}.

samples with an unsaturated linewidth of 0.1 mT at 30 mW incident microwave power and 1 s time constant of the detection channel.[14] When the InSb bolometer is used as a detector, the sensitivity is improved by a factor of 20.[13]

For ENDOR spectroscopy an NMR coil with two or four loops is incorporated just outside the resonator and energized by a 500 W rf amplifier. By means of a tuned rf resonance circuit, up to 1 mT B_2 field (rotating frame) can be achieved at the sample site. The microwave resonator and ENDOR coil are arranged in the bore of the cryomagnet in such a way that the B_0, B_1 and B_2 fields are mutually orthogonal.[6] A convection-type cooling system gives stable temperatures in the range of 30–300 K.

In the first experiments of this type, 3-mm ENDOR spectra were obtained from single crystals of γ-irradiated α-aminoisobutyric acid at 100 K[6] and of DANO (di-*p*-anisyl nitroxide) 1% in 4,4-dimethoxybenzophenone at 150 K.[11] Well-resolved structures from ^{1}H and ^{14}N dipolar and quadrupolar hf interactions were observed (see Fig. 7.4). Most recently, 3-mm EPR and ENDOR spectra of frozen solutions of semiquinone radical anions, related to photosynthesis, were recorded.[11] The EPR spectra are distinguished by well-separated Zeeman components with additional proton hf splittings. Fig. 7.5 shows a comparison of the EPR spectra of the simplest quinone, the benzosemiquinone radical anion, at X-band (3 cm) and W-band (3 mm), again demonstrating the improved resolution at high magnetic field.[11] Even for complex

systems, such as ubiquinone or vitamin K_1 occurring as acceptors in photosynthetic organisms, the spectral features belonging to g_{xx}, g_{yy}, g_{zz} are well-resolved at such high Zeeman fields so that they can easily be analyzed in terms of g- and hf-tensor interaction parameters.[11] The even smaller g-anisotropy of P^{+}_{865} in frozen RC solutions could be partly resolved.[11]

Extending ongoing X-band EPR/ENDOR/TRIPLE work on P^{+} in RC single crystals (see Section 3.2.1a), W-band EPR experiments on the light-induced P^{+}_{865} in single crystal RCs from *Rb. sphaeroides* R-26 have been performed recently.[11,15] First, the RC crystal was rotated in the Zeeman field with the crystal axis $z \parallel B_0$. Well-separated rotation patterns of the g-values of the remaining two magnetically inequivalent sites of the four RCs in the unit cell were observed. A preliminary analysis of the g-tensor values obtained yielded interesting information about the symmetry of the electronic structure of P^{+}_{865} which is complementary to the information extracted from the hf couplings. Extension of this work to 3-mm ENDOR is in progress in Berlin.

In another application of 3-mm EPR, the illuminated RC preparation of *Rb. sphaeroides* R-26 with the Fe^{2+} replaced by Zn^{2+} was studied.[11] The Zeeman magnetoselection at B_0 fields of 3.3 T was shown to be high enough to allow simultaneous detection of the EPR spectra of the donor and acceptor ion radicals, P^{+}_{865} and Q_A^{-}.

(c) Future Directions

The full exploitation of the resolution capability inherent in high-field EPR/ENDOR requires adequate detection sensitivity of the spectrometer. In principle, the sensitivity should significantly increase with increasing Zeeman field. In practice, however, existing high-field EPR spectrometers fall short of the theoretical sensitivity. The minimum detectable number of spins depends on the Zeeman frequency, the temperature, the sample volume, the Q-value and microwave coupling of the resonator, its filling factor, the EPR linewidth and field modulation amplitude, the noise figures and insertion losses of the microwave source, components and detector, the microwave power, the noise figure of the preamplifier, and the effective band width of the lock-in amplifier.[16] If one assumes that the microwave or FIR source, components, detection, and amplification stages are frequency-independent in their noise characteristics (which, in practice, is unrealistic, see below) simple expressions for the frequency dependence of the detection sensitivity can be deduced. For constant incident microwave power and unsaturated EPR lines, one obtains:[16,17]

(1) $N_{min}/V_s \propto \omega_e^{-3/2}$, for the minimum detectable spin concentration, when the sample size is scaled to the same extent as the cavity dimensions, i.e., when the filling factor remains constant (ω_e is the Zeeman frequency, V_s is the sample volume); and

(2) $N_{min} \propto \omega_e^{-9/2}$, for the minimum number of detectable spins when the sample size cannot be varied, i.e., when V_s is constant and the filling factor is proportional to V_s/V_c with the cavity volume V_c being proportional to ω_e^{-3}.

Case 1 applies to the experimental situation in which there is enough sample material available to be put into the cavity without appreciably lowering its Q-value; Case 2 corresponds to small single crystals. Thus, for the small-size RC single crystals, it should be very advantageous to perform high-field EPR also from the viewpoint of sensitivity. In practice, however, unfavorable noise characteristics of microwave and FIR components, such as sources and detectors, severely limit the actual sensitivity at ultra-high frequencies. Therefore, future technological developments of high-field EPR will be primarily concerned with improving the detection sensitivity. In particular, the signal-to-noise performance of Schottky detector diodes deteriorates significantly at mm wavelengths. InSb hot electron bolometers are a reasonable alternative when striving for the ultimate sensitivity theoretically attainable at the high Zeeman field employed.[3] In fact, such a bolometer is used as a microwave detector in a 150-GHz spectrometer[4] and a 95-GHz EPR/ENDOR spectrometer.[13] These devices require liquid He cooling, but their Noise Equivalent Power (NEP) for mm-waves is typically more than one order of magnitude lower than for Schottky detector diodes operating at room

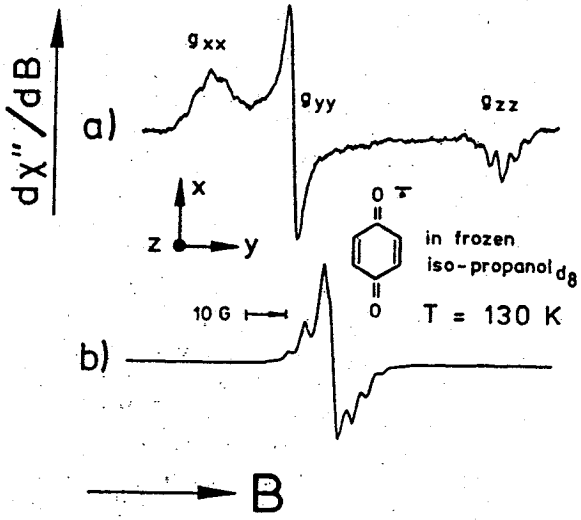

Fig. 7.5. Comparison of the resolution between W-band (a) and X-band (b) EPR spectra of the benzo-semiquinone radical anion in frozen perdeuterated iso-propanol.[11] In contrast to the unresolved spectrum at X-band, the W-band spectrum shows well-separated g-tensor components with resolved proton hf structure on the g_{xx} and g_{zz} peaks.

temperature (NEP [Schottky] = 2×10^{-12} W/$\sqrt{\text{Hz}}$ vs. NEP [InSb] = 10^{-13} W/$\sqrt{\text{Hz}}$).[3] InSb bolometers offer fast enough response times, τ, to accomodate high-frequency field modulation but, unfortunately, are too slow for high-performance pulsed EPR spectrometers (τ [Schottky] = 1 ns *vs.* τ [InSb] = 100 ns).[3] The trend of modern EPR spectroscopy to complement CW techniques with pulsed EPR (see Section 7.3.2) will certainly also be followed in the high-field/high-frequency domain. In fact, first pulsed EPR mm-EPR spectrometers have been constructed in a few laboratories.[4b,5b,7]

Site-selection in single crystals with complex unit cell composition is one of the promising applications of high-field EPR/ENDOR; precise *g*-value measurements in frozen disordered solutions of biomolecules is another. Well-resolved anisotropic Zeeman and hf interactions can serve as sensitive probes of pigment–protein interactions, such as hydrogen bonding to specific amino acid residues. For biosystems, these anisotropic interactions are often obscured at conventional X-band EPR spectroscopy.

The choice of an optimum frequency and field is, of course, significantly dependent on the actual detectable spin concentration that can be realized at that frequency. Also, one reaches a practical upper limit in available high-resolution superconducting magnets at about 14 T (corresponding to 0.7-mm wavelength for $g = 2$), although lower resolution Bitter Magnets can increase this range to about 22 T[18] (corresponding to $\lambda \approx 0.5$ mm).

Aside from these practical considerations, the choice of an optimum frequency and field depends on the details of the spectrum. Thus, if resolving power is of interest, one must consider the sources of linewidth. For rigid-limit spectra the important consideration is the extent to which *g*-strain (i.e., a distribution of *g*-values arising from inhomogeneity in the local environments of individual spin probes) determines the inhomogeneous linewidth compared to other sources (e.g., site variation in the hf tensor or unresolved hfs). As the field is increased, the *g*-strain contribution will ultimately become dominant and further increases in the field will not enhance EPR resolution. In many cases, EPR spectra from fluids will also be mainly inhomogeneously broadened, due to unresolved hfs, so similar comments would apply. In the case of radicals in fluid media with resolved hf spectra where the widths are homogeneous, the *g*-tensor contribution to the width would increase quadratically with the field until the onset of the slow-motional regime. Thus, while frequency dependent studies of motions can be very useful in the range where the *g*-tensor motional line broadening is dominant, there will be significant loss in signal sensitivity from the enhanced spectral widths.

7.3.2. TIME-RESOLVED CONTINUOUS WAVE- VS FOURIER TRANSFORM-EPR (H.L. AND D.S.)

Different types of time-resolved EPR methods currently being employed are relevant to photosynthesis:

1. **Light-modulation–field-modulation phase sensitive CW detection.**[19] This method suffers from a relatively low time resolution (~200 μs), dictated by the spectrometer's time constant being governed mainly by the field modulation (100 kHz) response time.
2. **Selective laser excitation CW-direct detection (DD).**[20] This fast EPR method allows investigation of time-dependent phenomena, where the transient magnetization (M_y) of the paramagnetic species, produced by light pulses, is monitored as a function of time, and/or the external magnetic field. In some cases, time together with microwave power dependence of the transient magnetization produces transient nutations. Magnetic field dependence of the transient magnetization provides spectral information as a function of time.
3. **Selective laser excitation-pulsed EPR spectroscopy,** in the most basic forms of Fourier Transform (FT) of the Free Induction Decay (FID) after a single-pulse excitation, or Electron Spin Echo (ESE) detection following a two microwave pulse excitation. While pulsed techniques represent the bulk of modern NMR spectroscopy, technical limitations associated with the considerably faster time range have delayed a parallel development in EPR spectroscopy. The overcoming of these technological difficulties within the last decade has led the way to considerable well-documented progress.[3,21]

   We will restrict the discussion here to techniques which are of relevance to photosynthesis.

The latter two methods avoid the constraints of field modulation, resulting in time resolution enhancement by three orders of magnitude down to less than 100 ns. Moreover, the two methods complement each other with inherent limitations and advantages. For example, microwave excitation of several hundred Gauss over a wide spectral range, typical of photoexcited triplets, is accessible to FT-EPR only inconveniently. On the other hand, triplets can readily be detected by CW-DD methods, with time resolution of ~100 ns. Radical species formed upon light excitation often cover a spectral EPR range of approximately 30 Gauss, and can be easily detected by FT (as well as CW-DD)-EPR methods. In this respect, the main advantage of using FT-EPR is the possibility of detecting transient radicals within a few nanoseconds (~10 ns) after laser excitation. Thus, the time window

between 10 and 200 ns becomes operational by the employment of FT-EPR or field-swept spin echo methods.

Since most EPR laboratories are equipped with CW spectrometers, it is noteworthy that a serious drawback of CW-DD method is possible misinterpretation of the early time spectra of small hyperfine splittings and narrow linewidth,[22] due to the appearance of Torrey wiggles at off-resonance fields. At short times, the spins precess, as described by the Bloch equations, about the effective magnetic field, which is the vector sum of the microwave field and the resonance offset. This precession produces transient signals for a time ~T_2 on either side of each hyperfine line. Thus, at times shorter than T_2, this effect produces spectra which have a very different appearance than spectra of the same radicals at longer times. We emphasize this point since the experimental results which exemplify the theoretical predictions are scarce, and a relevant example was mentioned earlier (see Section 6.5.3).

Within the context of photo-induced intermolecular ET reactions involving triplet porphyrins (or chlorophylls, Chls) as precursors (donors), and conventional quinones (donors) both methods of detection are essential and complementary.[23] In reactions with radical-ion products of small hyperfine coupling constants and narrow line widths (e.g., quinones), it has been demonstrated that the pulsed microwave method is more advantageous.[22c,24] Nevertheless, one has to consider also that the excitation bandwidth of pulsed EPR is presently limited to several hundred MHz, insufficient for many EPR applications, again particularly in the slow motion regime typical for RC investigations. In summary, typical EPR applications exist in most photosynthetic RC studies, where the DD-EPR detection offers advantages as a complementary rather than competing technique to the pulsed EPR methods. It is for these reasons that FT-EPR has not been applied yet in natural photosystems. In addition, much less demanding technical and instrumental requirements mean an easier realization of DD-EPR in high-field EPR.

7.3.3 2-D EPR (J.H.F. AND D.G.)

In the study of photosynthesis one investigates several different phenomena, including motional processes such as electron transfer (ET), and effects of static magnetic interactions such as electron spin polarization in triplet states. Our purpose here is to describe the potential of some modern EPR techniques, the so called "two dimensional EPR" techniques, with which one may study both interactions, ranging from about 10^{-2} MHz to about 10^{2} MHz, and various processes on time scales of between 10^{-4} sec and 10^{-11} sec. Information on both interactions and dynamics can be obtained from the "two dimensional" lineshapes directly, rather than indirectly as in conventional experiments.

Over the last several years an extensive range of experiments based on electron-spin-echo (ESE) and Fourier Transform (FT) techniques for the study of spin relaxation and motional dynamics of spin probes and spin-labeled macromolecules has been developed.[25] Modern 2-D ESE methods provide a 2-D display of the homogeneous lineshapes across an inhomogeneous EPR spectrum,[26] or of the cross-relaxation rates from each point in the spectrum.[27] They have greatly enhanced the sensitivity of EPR to motional dynamics, as demonstrated in a variety of 2-D experiments on spin-labeled model membranes and proteins.[25,28-30]

Even more dramatic has been the introduction of 2-D FT-EPR spectroscopy.[25,27,31-33] Instead of looking at a single (motionally narrowed) peak of an EPR spectrum, it has become possible to obtain a 2-D display of "autopeaks" and of "cross-peaks" whose intensities relate directly to cross relaxation phenomena such as Heisenberg spin Exchange (HE) and/or intermolecular Electron–Electron Dipole (EED) interactions modulated by translational diffusion, as well as intramolecular electron–nuclear dipole (END) interactions modulated by rotational diffusion.

This 2-D FT-EPR has recently been extended to the slow-motional and rigid limit regimes,[34,35] greatly enhancing their applicability to a broad range of biological samples. The ability to cover the entire spectral range of a slow-motional spectrum, for example, leads to a complete 2-D mapping of the (integrated) transition rates between all the points in the spectrum.[35] This type of 2-D exchange spectroscopy is the epitome of the Electron–Electron Double Resonance (ELDOR) approach originally pioneered by Hyde, Chien, and Freed.[36,37] We refer to it as "2-D ELDOR". It enhances the sensitivity, reliability, and accuracy with which EPR may be applied to questions of dynamics and molecular structure in physical research. Relevant dynamic processes in photosynthetic systems that can be studied by 2-D ELDOR include rotational diffusion, Heisenberg spin-exchange, chemical exchange, and ET.

(a) Motional Studies

One of the fundamental problems of CW-EPR for motional studies has been its rather low resolution as regards the details of dynamics. The spectral parameter that reflects the motional dynamics is the homogeneous T_2, which is the inverse of the homogeneous linewidth. In the case of strong inhomogeneous broadening, the inverse inhomogeneous linewidth T_2^* is much shorter than T_2. Thus, in the very slow-motional regime (i.e., for rotational correlation times $\tau_R > 10^{-7}$s for nitroxides), where the EPR spectrum of nitroxide spin labels ap-

proach a broad, inhomogeneous rigid-limit pattern, CW-EPR is relatively insensitive to the details of the dynamics. Even for faster motions, the inhomogeneous broadening by proton (and/or deuteron) superhyperfine splittings obscures the dynamic contributions to the observed lineshapes. These factors have reduced the sensitivity of CW-EPR studies in the past, especially in biological systems, which tend to exhibit larger inhomogeneities and slow motions.

The initial approach to resolving homogeneous T_2s has been to use the electron spin-echo (ESE) technique,[24-27,38-40] which effectively cancels out the inhomogeneous T_2*. In the case of slow motional spectra, T_2 is always much longer than T_2*,[31] so that much slower motions can be detected by spin-echo methods than by CW-EPR.

In order to maximize the information obtained from studying T_2, a field-swept 2-D ESE technique (Fig. 7.6) was introduced which provides a simple map of the homogeneous T_2 across the spectrum (Fig. 7.7). This technique has been used for a wide range of sample conditions, including studies of viscous fluids,[26] oriented model membranes,[28] and spin-labeled proteins.[29,30] These studies have demonstrated that "T_2-plots" are not only very sensitive to motion in the region $10^{-7} < \tau_R < 10^{-4}$ s, but also to the specific models for rotational reorientation. In particular, they provide clear distinctions of isotropic vs. anisotropic motions, even when such information cannot be reliably obtained by CW-EPR (Fig. 7.8).

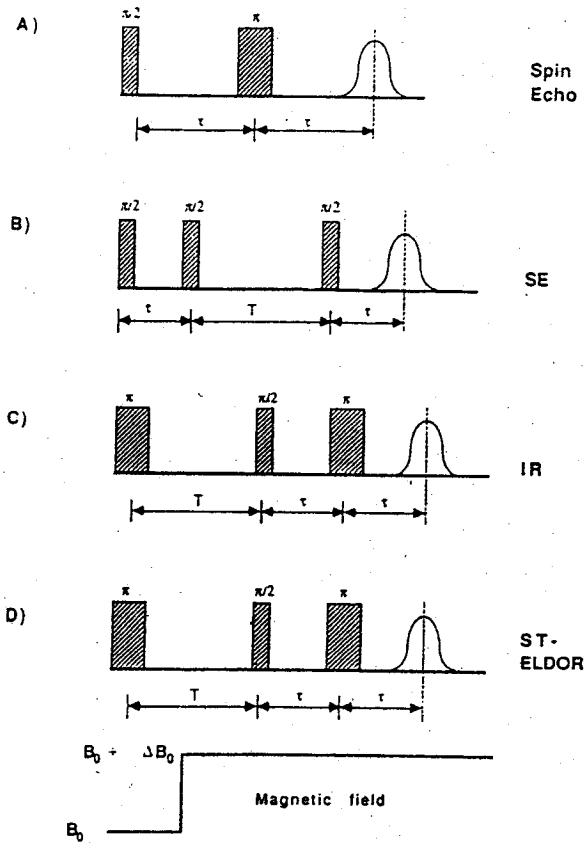

Fig. 7.6. Typical spin echo pulse sequences: (a) Hahn spin echo; (b) Stimulated Echo; (c) Inversion recovery; (d) ST-ELDOR echoes. From ref 25.

A further application of 2-D ESE methods is the study of slow-motional dynamics by T_1-type experiments. In general, the rate of magnetization transfer (MT) out of each spectral region should vary across the spectrum in a way that could be more sensitive to molecular motion than the T_2-type experiment just described.[25,26] A field-swept 2-D ESE MT experiment based upon the three pulse stimulated echo sequence (cf. Fig. 7.6) has been demonstrated in model studies, and it showed dramatic evidence for very anisotropic rotation (Fig. 7.9). It appears that rotational motions are detectable at lower temperatures than with T_2-type 2-D ESE experiments.

A major limitation of the field-swept methods described above is the long data-acquisition periods required, because one sweeps the field through the spectrum, collecting the echo envelope decay at each spectral position. This limitation makes the method impractical for many types of biological samples where the small spin concentrations require extensive signal averaging. Much more rapid data acquisition would be possible if one were to irradiate the whole spectrum and collect the entire FID (or the echo shape) with each pulse sequence. Such ideas are completely analogous to NMR, where FT and 2-D FT methods have been well developed.

FT-EPR presents major instrumental challenges compared to FT-NMR. The time-scale of electron spin relaxation is on the order of ns, compared to ms for nuclei. Moreover, even motionally-narrowed nitroxide EPR spectra extend over about 100 MHz, requiring time resolution of at least 10 ns (with quadrature detection) and narrow intense pulses. Finally, microwave technology is more complex than the equivalent rf technology.

FT and 2-D FT EPR techniques have been extensively developed at Cornell.[25,31-35,41-43] This major breakthrough in EPR spectroscopy may be expected to revolutionize the biomedical applications of EPR, much as it did for NMR. Initial experiments were on motionally-narrowed nitroxide spin labels, especially the 2-D ELDOR method noted above. In this technique, off-diagonal, or cross-peaks appear, which measure magnetization transfer by spin relaxation processes. These are the "ELDOR peaks", which are frequency-discriminated from the main, diagonal peaks (Fig. 7.10). The principal spin relaxation mechanisms are HE and END interactions leading to nuclear spin-flip transitions (with rate W_e). The pattern of the cross-peaks helps to distinguish which relaxation mechanism is dominant. The quantitative accuracy of these

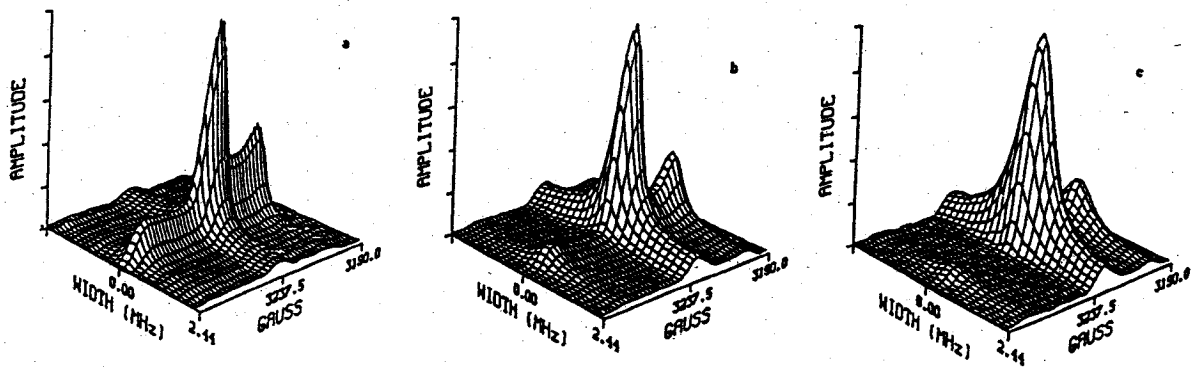

Fig. 7.7. Two-dimensional spectra for Tempone in 85% glycerol/H2O at (a) –100° C, (b) –75° C, (c) 65° C, after Fourier filtering and Fourier transforming. From ref 33.

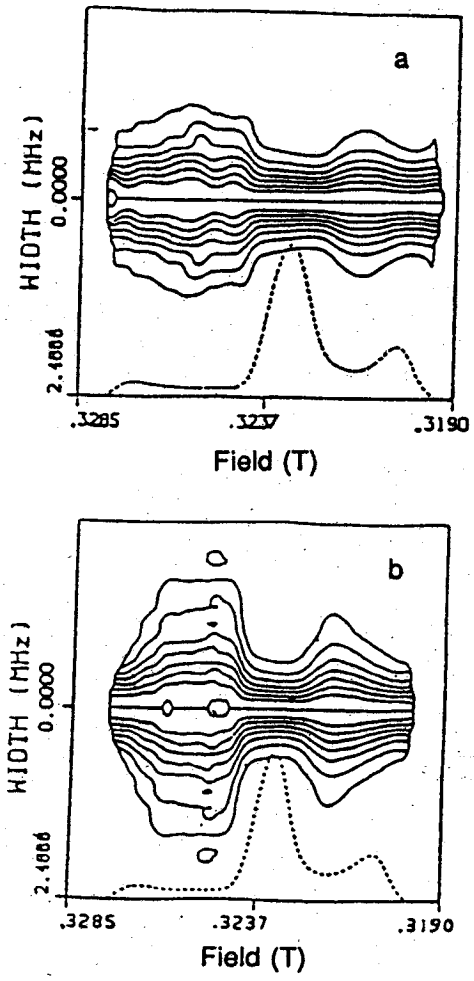

Fig. 7.8. Normalized contours and 0 MHz slices from spectra of two different nitroxides: (a) The spectrum of Tempone in 85% glycerol/H2O at –75° C; (b) The spectrum of CSL in *n*-butylbenzene at –135° C. The T_Ms for these spectra, under these conditions, are approximately the same. From ref 33.

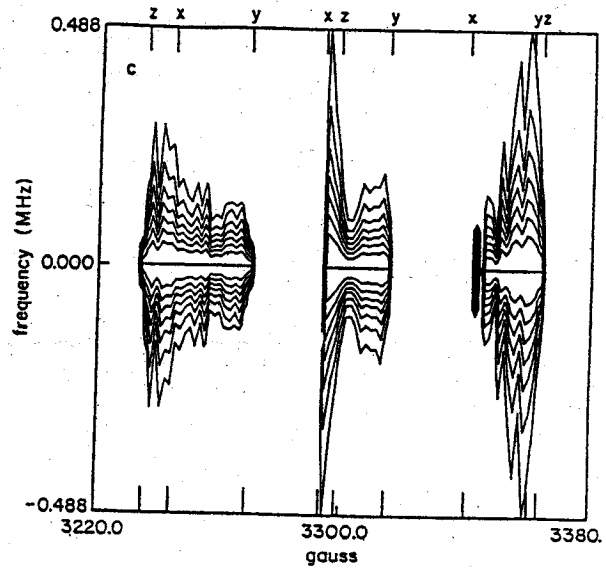

Fig. 7.9. Two-dimensional ESE contours from stimulated echo sequence for NO_2 on vycor at 35 K showing rates of magnetization transfer. It shows relatively rapid rotation about the molecular *y* axis (i.e., the axis parallel to oxygen–oxygen internuclear vector). From ref 33.

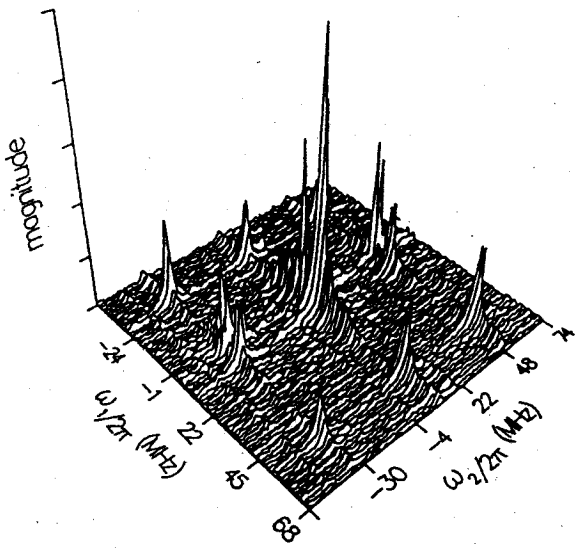

Fig. 7.10. Absolute value 2-D ELDOR spectrum of 1.17×10^{-3} M PD-Tempone in toluene-d_8 at 21° C; τ_p = 15.2 ns; Δt_1 = 6 ns; Δt_2 = 3.9 ns; 90 steps in t_1; 16-step phase-alternation sequence with 30 averaged FID per step; deadtime in t_2, 100 ns; deadtime in t_1, 120 ns; mixing time, $T = 3.10 \times 10^{-7}$s; 256 complex data points per FID extending to 1 μs; acquisition time, 27 min. From ref 33.

experiments was demonstrated in a study of HE.[25,32]

The extension of 2-D FT methods, including 2-D SESCY (two dimensional spin-echo correlation spectroscopy) and 2-D ELDOR, to the slow-motional and rigid limits regimes required several instrumental improvements, including extension of the spectral bandwidth to 200–250 MHz and sub-nanosecond time resolution of the echo decays. These initial experiments demonstrate the potential applicability of 2-D FT EPR methods to a broad range of biological samples which typically exhibit slow-motional behavior.

The 2-D SECSY experiment is the FT version of field-swept ESE, and provides a similar map of the homogeneous T_2 across the spectrum (Fig. 7.11) while dramatically reducing the data collection time.[34] In addition, 2-D SECSY provides structural information from nuclear modulation of the echo envelope as discussed below.

Under slow-motional conditions, 2-D ELDOR produces a continuum of cross-peaks corresponding to the transfer of magnetization from one spectral region to another by molecular reorientation.[35] We can observe that these "rotational cross-peaks" in different spectral regions grow at different rates with respect to the mixing time, thus revealing a detailed picture of rotational diffusion (Fig. 7.12).

The improved sensitivity of the new 2-D methods to molecular motion has provided a new means of resolving EPR spectra from species with different mobilities, e.g., bound vs. unbound substrates, or mobile vs. immobile membrane components. Given that the T_2s of two species differ because of their different mobilities or ordering, it is possible to use 2-D methods to unequivocally separate the two spectra according to their different T_2 s ("T2 discrimination") as has been shown on model systems.[40] Both the 2-D ESE techniques[25] and the newer 2-D SECSY-EPR (a two-pulse 2-D FT-EPR experiment) method may be employed to "T_2-discriminate" superimposed spectra from a wide variety of samples.

A particularly intriguing new application of 2-D ELDOR would be to measure reliably and accurately the exchange rates of radicals between different chemical environments in a sample, even under equilibrium conditions. Examples of such processes include substrate binding and release, enzyme-catalyzed chemical reactions, molecular transport across membranes, macromolecular aggregation, and exchange between different membrane phases. The 2-D ELDOR time scale of approximately 10^{-6} sec is ideally suited for examining such processes, and the recent extension of 2-D ELDOR to the very slow-motional regime[35] seems most appropriate for such work.

Two-dimensional FT methods should be particularly applicable to investigations of the electron spin polarization that is associated with the initial photochemistry of the RC. Spin polarized radical pair states have been observed both in photosystem I[44] and the bacterial RC.[45] In bacteria, the polarization arises during the series of reactions:

$$(P\,I\,Q) \rightarrow (P^{+}\,I^{-}\,Q) \rightarrow (P^{+}\,I\,Q^{-})$$

where P is the primary electron donor and I (pheophytin) and Q (quinone) are the primary and secondary acceptors, respectively. The polarization that is observed in the long-lived $(P^{+}\,I\,Q^{-})$ state has been explained as the result of either (1) a chemically-induced dynamic polarization (CIDEP) mechanism that takes place during the short-lived $(P^{+}\,I^{-}\,Q)$ precursor state;[46] (2) the presence of a constant (coherent) spin–spin interaction in the singlet-correlated $(P^{+}\,I\,Q^{-})$ radical pair;[47] or (3) some combination of these two mechanisms.[48] 2-D FT methods, in particular 2-D methods that select electron double-quantum coherence (see Section 7.3.3b) can be used to determine spin–spin interactions in the $(P^{+}\,I\,Q^{-})$ radical pair directly. Not only do such experiments afford the possibility of a structural determination for the $(P^{+}\,I\,Q^{-})$ state, they may also permit other relevant kinetic parameters of the dynamic polarization mechanism to be determined with greater accuracy than is possible from the CW-EPR spectrum alone. In addition, 2-D SECSY methods can provide a direct and accurate measurement of T_2 varia-

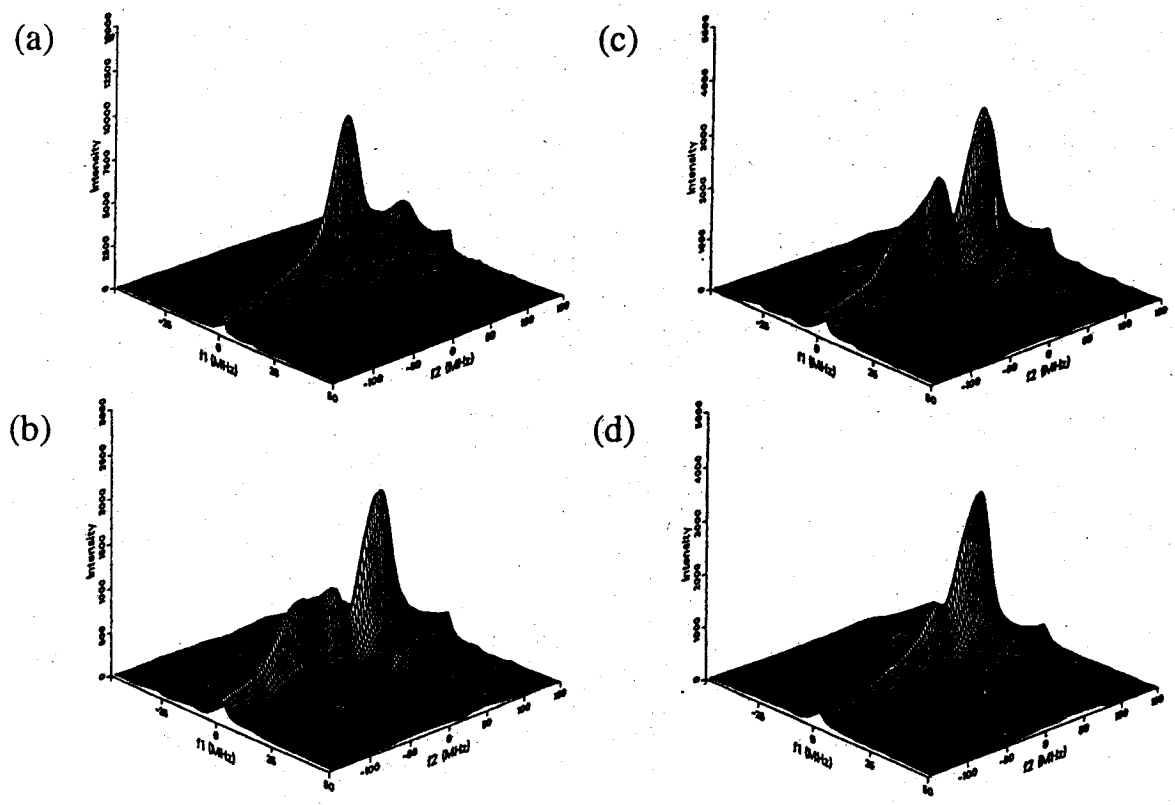

Fig. 7.11. Experimental SECSY-ESR spectra for (a) PD-Tempone at –103 °C and for ^{15}N-Tempone at the following temperatures: (b) –103 °C, (c) –83 °C, (d) –63 °C. These spectra have been processed by computational methods as explained in ref 34 (in relation to eq 2 there).

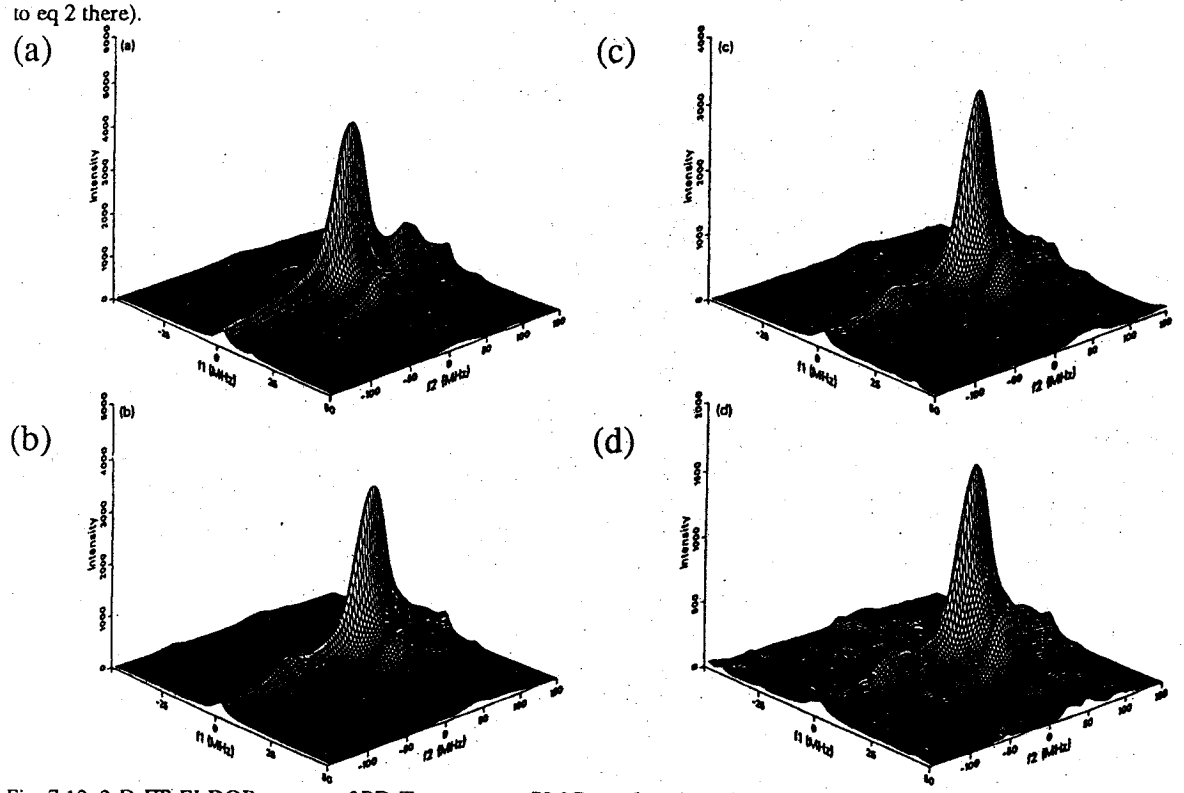

Fig. 7.12. 2-D-FT-ELDOR spectra of PD-Tempone at –73 °C as a function of the mixing time (a) T = 3 μs, (b) 20 μs, (c) 30 μs, (d) 40 μs. These spectra have been processed by computational methods.[34] Other experimental conditions are described in ref 35.

tion across the spectrum of the radical pair, which may be used for "T_2-discriminating" the spectra from the individual radicals. A particularly interesting system to study by 2-D FT methods would be RCs in which the Q acceptor has been pre-reduced, so that photoexcitation produces the 3-spin system ($P^+ I^- Q^-$). In this system, it has been observed that spin polarization developed in the ($P^+ I^-$) pair is transferred to Q^- by spin–spin interactions between I^- and Q^-.[49] Although the various magnetic and kinetic parameters of the system contribute to the CW-EPR spectrum in a complicated way,[50] specific interactions can be selectively studied by 2-D FT-EPR. For example, at low temperatures, the ($P^+ I^-$) state may be sufficiently long-lived to permit application of a 2-D ELDOR pulse sequence that would permit a direct measurement of the rate of magnetization transfer to Q^-.

Similar considerations apply to 2-D FT investigations of spin-polarized radical pairs in Photosystem I, although the reaction scheme (including reaction rates and the number and order of the electron acceptors) is not yet as well characterized as in bacterial RCs. ET reactions generally take place on a somewhat slower timescale that the bacterial reactions, making them more amenable to 2-D FT-EPR at higher temperatures. Thus, for example, it may be possible to apply 2-D ELDOR to uniquely identify kinetic pathways by the appearance of cross-peaks in the 2-D spectrum.

One-dimensional FT-EPR methods have already been extensively applied to photosynthetic model systems, taking advantage of their time resolution to follow the course of spin polarization that arises during ET and triplet energy transfer processes (as reviewed by Levanon in ref 23). Most recently, model compounds have been synthesized which should be especially amenable to study by the more sophisticated 2-D FT techniques. These compounds exhibit many of the ET properties of RCs, including high quantum yield charge separation at cryogenic temperatures, and the appearance of a spin-polarized radical pair EPR spectrum.[51] The compounds consist of a Zn-porphyrin primary electron donor situated between a naphthoquinone acceptor and a N,N,N',N' tetraalkyl phenylenediamine secondary donor; upon photoexcitation, they undergo a two-step ET process that produces a radical pair state with a 23 Å spin–spin separation and a 4 ms lifetime. By analogy with the ($P^+ Q^-$) radical pair in RCs, detailed structural information about the radical pair state of such model compounds can be obtained by 2-D FT spectroscopy; in particular by using double-quantum selective pulse sequences to map the electron spin–spin interaction across the EPR spectrum. Such studies would be especially useful for investigating the detailed orientation dependence of electronic interactions in model donor–acceptor complexes.

(b) Structural Studies

It is frequently difficult for CW-EPR methods to resolve the electron-nuclear hyperfine coupling of the radicals typical of photosynthetic systems which are useful for structural studies. Not only are such radicals characterized by numerous unresolved hf interactions, the large degree of inhomogeneity in biological systems often further obscures these interactions. For structural studies in the rigid limit, 2-D SECSY experiments provide significantly greater sensitivity to nuclear modulation patterns arising from the electron nuclear hf interactions than both CW-EPR and conventional ID electron-spin-echo envelope modulation (ESEEM) techniques.[33,52] In particular, in a study of the 2-D nuclear modulation patterns from nitroxide probes, it was possible to discriminate among several structural models by utilizing spectral simulations[34] (Fig. 7.13). These hf interactions may be used to map accurately the local nuclear structure near the unpaired electron due to their $1/r^3$ dependence, and due to the dependence of modulation on the number of nuclei involved.

The high sensitivity of 2-D SECSY techniques to hfi tensors will be particularly useful for organic radicals such as Chls, pheophytins, and quinones, which have large numbers of hf interactions that are unresolved by CW-EPR. Some particular areas of interest are:

1. comparative studies of proton tensors in the Chls of the primary electron donor, P, vs. those of Chl monomers in vitro (this has been thoroughly carried out previously by ENDOR, but would be useful for comparison);
2. careful comparative 2-D FT structural studies of the primary donor between different species of photosynthetic bacteria, and between these systems and higher plant photosystems I and II;
3. characterization of the secondary donor in photosystem II (Z), thought to be a tyrosine radical on the basis of ENDOR studies;
4 resolution of proton hfc tensors in single crystals of photosynthetic RCs, including those of the primary donor, and the pheophytin and quinone acceptor molecules.

Aside from accurately determining the structures of the radicals themselves, one could hope to identify specific protein-radical interactions.

Perhaps even more important, 2-D SECSY and related methods bring a significant new capability to EPR for structural studies. 2-D techniques are now routinely used in FT-NMR studies to detect dipole–dipole couplings among networks of nuclei, which can be used to map internuclear distances and determine local structural features of macromolecules.[53,54] Similarly, 2-D FT-EPR can

be used to map distances between electron spins. Because of the much larger distances over which electronic interactions extend, it should be possible to map the subunit structure of proteins and other macromolecular assemblies. 2-D FT-EPR methods thus afford a new means of structural determination on distance scales inaccessible by NMR, and with potentially greater accuracy than methods such as fluorescence energy transfer (FET). In fact, distances measured by FET suffer from large uncertainties in the K^2 parameter that describes the relative orientation of the transition dipoles of the two chromophores.[55] No such problem exists in EPR since the spins are quantized along the applied magnetic field.

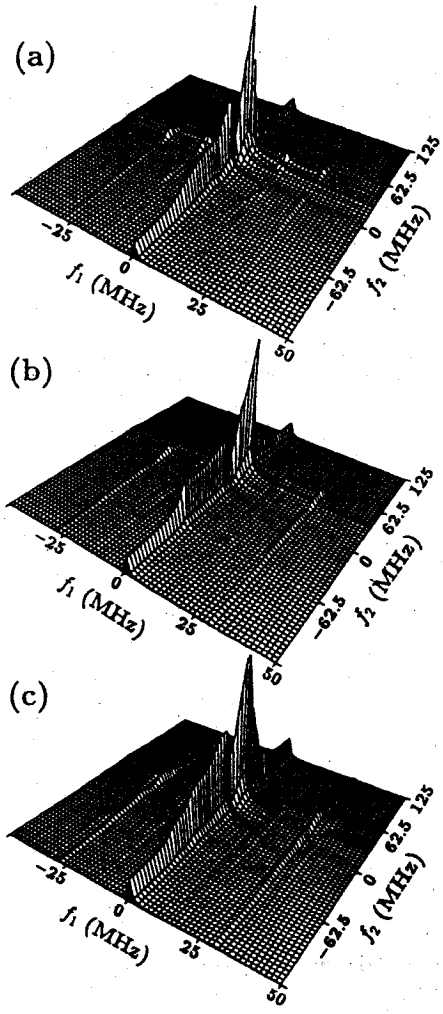

Fig. 7.13. Simulations of SECSY-EPR spectra in the rigid limit for ^{15}N-Tempone for several models of the geometric arrangement of the protons: (a) 12 completely equivalent methyl protons; (b) four groups of three completely equivalent methyl protons (see ref 34); (c) same as (b) but with an H-bonded water molecule. The methyl proton axial hf tensor used was $a = -1.2$ MHz and $D = -6.2$ MHz, which for (b) and (c) had polar angles with respect to the ^{15}N hf tensor of $\theta = 67°$ and the four values of $\phi = 55°$, 125°, 235°, and 305°. For the two H-bonded water protons in (c) we used $a = 0$, with $D_1 = 20$ MHz, $\theta_1 = 180°$, $\phi_1 = 0$ and $D_2 = 9$ MHz, $\theta_2 = 140°$, $\phi_2 = 90°$. From ref 34.

7.3.4 MAGIC ANGLE SPINNING (MAS)-NMR OF BACTERIAL REACTION CENTER (A.J.H.)

High-resolution NMR of proteins in liquid solution is possible for molecular weights not exceeding about 20 kD. Beyond that weight, the rotational correlation times become too large and incomplete averaging of dipolar interactions gives rise to severe line broadening, obscuring the individual resonances. A few years ago a technique was developed to circumvent this problem called magic angle spinning (MAS)-NMR:[56] a probe is spun at high frequency (typically 5 kHz) at an angle with the magnetic field of $\theta = 54°44'$. At this angle, the z-component of the dipolar interaction (which is proportional to $3\cos^2\theta - 1$) is zero. The result is an averaging of the dipolar interaction comparable to that in solution, and consequently a near restoration of high-resolution conditions (narrow lines).

^{13}C-MAS-NMR at 400 MHz has recently been applied to RC of *Rb. sphaeroides* R-26 in which all tyrosines were replaced by tyrosines labeled with ^{13}C at the 4'–C position (the carbon next to the hydroxyl group).[57a] Replacement was carried out by growing the bacteria on a synthetic medium containing 4'–^{13}C tyrosine. Employing proton-^{13}C cross polarization to enhance the sensitivity, difference ^{13}C-NMR of the labeled RC and native RC revealed a strong ^{13}C resonance of the tyrosyl residues, which could be resolved into two major bands containing 8 and 17 tyrosines, respectively, and two minor bands and one shoulder each representing a single tyrosine. The two resolved minor bands were provisionally attributed to tyrosines subjected to ring current shifts of adjacent BChl or BPhe macrocycles. The two major bands of 8 and 17 tyrosines were provisionallly attributed to tyrosines in a non-polar (intramembrane) and polar (extramembrane) environment, respectively. See also ref 57b.

The above experiment has shown that high-resolution NMR of a protein of molecular weight >90 kD is feasible. This offers a unique possibility to study amino acid environments and protein conformational changes, resulting for example from charge separation, on an atomic scale with a resolution significantly higher than that of X-ray crystallography. As a first result it was noted that, at ambient pH, all tyrosines were protonated.

To exploit MAS-NMR fully, resolved resonances should be firmly assigned to individual amino acids. Site-directed mutagenesis is an ideal tool for this and is currently in progress. The technique is of course not confined to ^{13}C-labeled tyrosines; preliminary results with ^{15}N-tryptophanes are promising. If successful, this